Wavelet-Based Image Registration Techniques: A Study of Performance

Nagham E. Mekky[†], F. E.-Z. Abou-Chadi[††], and S. Kishk[††],

[†]Misr Higher Institute for Engineering and Technology, Mansoura, Egypt
[††]Dept. of Electronics and Communications Engineering, Faculty of Engineering, Mansoura University, Mansoura, Egypt

Summary

This paper presents a comparative study of performance for four wavelet-based multiresolution image registration techniques. The proposed algorithms are implemented and applied to dental panoramic X-ray images and magnetic resonance (MR) images of the brain. Cross-correlation based registration, mutual-information (MI) based hierarchical registration, scale invariant feature transform (SIFT) based registration, and hybrid registration approach using MI and SIFT operator combined with wavelet-based hierarchical pyramid, have been utilized. A comparison between proposed techniques with the corresponding techniques in the spatial domain is achieved. The quality of the registration process was measured using the following criteria: normalized cross-correlation coefficient (NCCC) and percentage relative root mean square error (PRRMSE). The application of the selected techniques to dental panoramic X-ray images and brain MR images has shown that wavelet-based hierarchical approach combining MI, SIFT, and RANdom Sample And Consensus (RANSAC) algorithm gives the best results and can be used efficiently for registration of two types of images.

Key words:
Dentistry, hybrid approach, magnetic resonance (MR), mutual information, and wavelet pyramid.

1. Introduction

Image registration is an important step in maximizing the information embedded in imaging datasets. Registration aims to spatially match datasets that may differ in time of acquisition, imaging device, and acquisition angle. After registration, spatial correspondence between functional information and anatomical structure can be achieved. Medical image registration techniques can be classified into feature-based, intensity-based, and hybrid methods [1].

In feature-based registration approaches, the features can be extracted manually or interactively. One main advantage of feature-based registration is that the transformation often can be stated in analytic form, which leads to efficient computational schemes. However, in feature-based registration methodologies, the preprocess step is needed and the registration results are highly dependent on the result of this preprocess [2].

Fully and directly exploiting the image intensities, the intensity-based image registration algorithms have the advantages of no segmentation required and most importantly, these methods have potentials to achieve automated registration. However, the computation of this category of schemes not efficient. To improve the computational efficiency and registration accuracy on intensity-based registration, multiresolution registration have been proposed.

By combining intensity-based techniques with feature-based methods, hybrid registration approaches try to exploit the merits of both and at the same time avoid their disadvantages. Hybrid registration can be automatic, more accurate, and faster than either of its registration components used separately [3].

Scale invariant feature transform (SIFT) operator is a feature detector introduced in 1999 by Lowe [4] and improved in 2004 in [5]. Since its introduction, it has proven its effectiveness for numerous applications especially in the field of computer vision [4]. Therefore, the evaluation of SIFT operator descriptors in the field of dental panoramic X-ray and brain MR image registration becomes an interesting application.

By decomposing the datasets into multiple resolutions and performing the registration from low resolutions to high resolutions, hierarchal registration speed, avoid local minima, and therefore improve registration performance [6]. The performance evaluation of using wavelet transform combined with SIFT operator in the field of dental X-ray and brain MR image registration is not examined briefly in the literature.

The present study aims to select the best registration technique used to register images (reference image and recent image) for dental panoramic X-ray images and MR images of the brain. Four wavelet-based image registration methods were investigated: cross-correlation based registration, registration by maximization of MI, registration using SIFT features, and hybrid registration technique described in [7] combined with wavelet-based pyramid approach. The main objective is to investigate the

performance of the proposed methods with results obtained from the same algorithms in the spatial domain. Comparing the performance of these techniques has been achieved using two evaluation criteria: the normalized cross-correlation coefficient (NCCC) and the percentage relative root mean square error (PRRMSE).

2. Data Acquisition

Two sets of data images were used. X-ray and MR images are used in the present work to choose the most effective method for registering these images.

2.1 Dental Panoramic X-ray Imaging

Twenty-five panoramic X-ray image pairs were taken from the Department of prosthodontics, Faculty of Dentistry, Mansoura University. The images were taken from five patients, with a size of approximately 219 pixels by 368 pixels. The average time interval between the patient's radiography and the next one was 18 months (range 2-53 months). Fig. 1 illustrates an example of dental panoramic X-ray reference image and a recent image.

2.2 Magnetic Resonance Imaging (MRI)

The second set of images contains 54 brain MR images of size of 616 pixels by 595 pixels, taken from El-Mogy Radiography Center, Mansoura. These images were taken from three patients at different times. The average time interval between one image and the next was 3 months. Fig. 2 depicts an example of brain MR reference image and recent image.

3. The Methodology

Four image registration techniques were applied to both dental panoramic X-ray and brain MR images, based on wavelet decomposition. The first technique is based on cross-correlation [8]. The second one depends on maximizing mutual information (MI) using hierarchical approach [9]. The third technique is based on matching SIFT features [4] extracted from two pyramid images. The fourth one utilizes a hybrid approach combining MI and SIFT operator [7] using wavelet pyramid approach. Firstly a discrete two-dimensional (2D) wavelet decomposition was performed on two images, the reference image and the recent image, to the second level of resolution. Second, each image was then decomposed into approximation coefficients and detail coefficients matrices. Daubechies' 4-coefficient (db4) was chosen to decompose the two images because its ability of keeping energy in the low frequencies. Then each registration technique was applied on approximation coefficients of reference and recent

images. Finally, after finishing the registration steps, inverse discrete wavelet transform (IDWT) was applied in order to obtain the registered image [10].

4. Cross-Correlation Based Registration

Registration was implemented using Matlab 7.4. At the first decomposition level, the approximation coefficients of the reference image and the recent image have the highest normalized cross-correlation coefficient at exactly the displacement between the recent image and the reference one [8].

The two-dimensional normalized cross-correlation function between a reference approximation image f, and recent approximation image t, with means $\bar{f}$ and $\bar{t}$ respectively, was computed using:

$$K(u,v) = \frac{\sum_{x,y}[f(x,y)-\bar{f}_{u,v}][t(x-u,y-v)-\bar{t}]}{\sqrt{\sum_{x,y}[f(x,y)-\bar{f}_{u,v}]^2[t(x-u,y-v)-\bar{t}]^2}} \tag{1}$$

where x, y are the pixel coordinates, u, v refer to the shift at which the cross-correlation coefficient is calculated. Having this displacement, the approximation coefficients of the recent image is easily warped to approximation coefficients of the reference one.

(a)   (b)
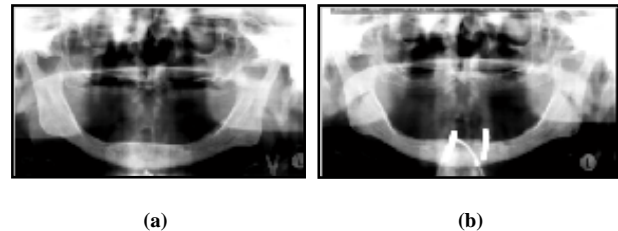
Fig. 1 An example of dental panoramic X-ray (a) reference image and (b) recent image.

(a)   (b)
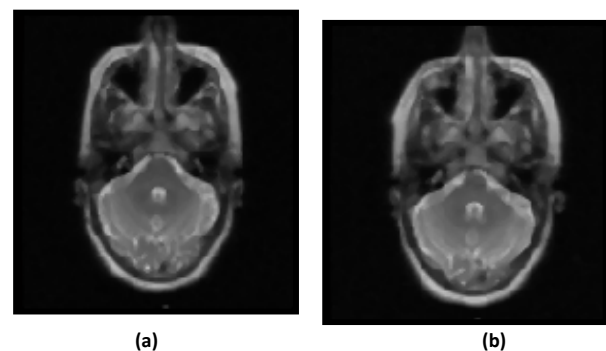
Fig. 2 An example of MR images of the brain (a) reference image and (b) recent image.

5. Mutual-Information-Based Hierarchical Registration

Mutual-information based registration has the property of high precision, but it is also time consuming. Therefore, to improve the computational efficiency, the images were registered from low resolution (high level) of the registration pyramid to high resolution (low level) of the registration pyramid.

The entropies of approximation coefficients of both reference and recent images were calculated as well as their joint entropy. Then the mutual information (MI) of two images A and B was calculated as follows [11]:

$$MI(A, B) = H(A) + H(B) - H(A, B) \qquad (2)$$

where A denotes the reference approximation image, B refers to the recent approximation image, while $H(A,B)$ is their joint entropy and $H(A)$, $H(B)$ are the entropies of A and B respectively.

In each hierarchy, an affine transformation between the approximation coefficients of both reference and recent images was applied as [9]:

$$\begin{bmatrix} x_2 \\ y_2 \end{bmatrix} = \begin{bmatrix} a_{13} \\ a_{23} \end{bmatrix} + \begin{bmatrix} a_{11} & a_{12} \\ a_{21} & a_{22} \end{bmatrix} \begin{bmatrix} x_1 \\ y_1 \end{bmatrix} \qquad (3)$$

where pixel (x_1, y_1) in recent approximation image I_1 is mapped to the pixel (x_2, y_2) in reference approximation image I_2. The coefficients (a) parameterize the six degrees of freedom of the transformation. In order to maximize mutual information, an adaptive search for optimum transformation parameters was performed.

6. Image Registration Using Sift Features

Scale Invariant Feature Transform (SIFT) approach utilized by Lowe [4] was performed to detect and extract distinct features from both reference and recent approximation images at the first pyramid decomposition level. These features were used to perform matching between registered images. Four steps for image registration using SIFT features have been applied: extraction of SIFT features, matching of SIFT features, removal of outliers, and selecting the transformation model between two images and estimating its parameters. The last two steps were combined in this work because the outlier detection was part of the parameter estimation procedure using RANdom Sample and Consensus (RANSAC) algorithm.

6.1 Extraction of SIFT Features

Keypoints for SIFT features correspond to scale-space extrema at different scales. Therefore, the first step towards the detection of extremas was filtering the images with Gaussian kernels at different scales. The difference of Gaussian (DoG) filtered images of adjacent scales were generated as follows [5]:

$$L(x, y, \sigma) = G(x, y, \sigma) * I(x, y) \qquad (4)$$

$$D(x, y, \sigma) = \big(G(x, y, k\sigma) - G(x, y, \sigma)\big) * I(x, y) \qquad (5)$$

where I is the image, G the Gaussian kernel and L the scale-space image generated by convolution (*). D represents the difference of Gaussian (DoG) filtered images.

The filtered images were organized an image pyramid in which the blurred images were grouped by octave. An octave was corresponded to doubling the sigma (σ) value of the Gaussian kernel. On each image scale (octave), a fixed number of blurred images (sub-levels) was created. In this study, 3 octaves with 6 differently blurred images on each octave was used.

In order to detect the local maxima and minima of the DoG images across scales, each pixel in the DoG images was compared to its eight neighbours in the current image and the nine neighbours in the neighbouring (higher and lower) scales. If the pixel was a local maximum or minimum, it has been selected as a candidate keypoint.

The SIFT descriptor is a weighted and interpolated histogram of the gradient orientations and locations in a patch surrounding the keypoint. In order to determine the keypoint orientation, a gradient orientation histogram has been computed employing the neighbourhood of the keypoint. Each neighbouring pixel was contributed by its gradient magnitude to determine the keypoint orientation. Keypoints with low contrast have been removed and the responses along edges have been eliminated. All the properties of the keypoint have been measured relative to the keypoint orientation. This provided invariance to rotation. The histograms contained 8 bins each and each description contained an array of 4 histograms around the keypoint which leaded to a SIFT vector of 128 elements [4, 5].

6.2 Matching of SIFT Features

The matching process was performed based on wavelet-based hierarchical pyramid for both reference and recent images. At the first level of the reference and the recent

pyramids, each feature point within the wavelet domain of the recent image is searched for within the wavelet domain of the reference image.

In the matching stage, the descriptor matrices of reference and recent approximation images have been compared. The matching was based on the idea of finding the nearest neighbours in the descriptor matrices. For robustness reasons the ratio of the nearest neighbour to the second nearest neighbour was used.

The Euclidean distance was given by [4]:

$$\|y - z\|_2 = \left(\sum_{i=1}^{B}(y_i - z_i)^2\right)^{1/2} \qquad (6)$$

where y and z are two descriptor vectors. The inner product of the vector (y - z) with itself

$$(y - z) \circ (y - z) = y \circ y + z \circ z - 2|y||z| \cos(\angle(y, z)) \quad (7)$$

showed that, with normalized vectors y and z (length 1) the angle

$$\alpha = \arccos(\angle(y, z)) \qquad (8)$$

can be used as a good approximation within the minimum search, in particular for small angles. For each target descriptor, the first and second nearest descriptors have been found. A pair of nearest descriptors gave a pair of matched keypoints, if the ratio between the distances to the first and second nearest descriptors have been lower than a given threshold (t). A matching threshold of 0.8 has been applied.

6.3 Removal of Outliers Using RANSAC

A RANdom Sample And Consensus (RANSAC) algorithm proposed by Fischler and Bolles [12], was utilized. It has been used to remove outliers automatically and estimate similarity (linear conformal) transformation parameters between two approximation images. The basic RANSAC algorithm consists of the following steps that were iterated over.

1) RANdomly select minimal sample sets (MSS) from the input dataset. (The size of the MSS is the smallest number sufficient to estimate the similarity transformation model, which in this case is 2). Compute the model parameters using only the MSS.

2) For the computed model, classify the other data points (outside the MSS) into inliers and outliers. The set of inliers constitutes the consensus set (CS).

These two steps were iterated over till the probability of finding a better CS drops below a certain threshold. The model that gave the largest cardinality for the CS was taken to be the solution. After estimating the parameters between the images, the recent approximation image was re-sampled to the resolution of the reference approximation image using bilinear interpolation.

7. The Proposed Technique

The proposed registration technique combines MI and SIFT operator based on wavelet decomposition. Fig. 3 depicts the framework of the proposed methodology. For dental panoramic X-ray images and brain MR images, the SIFT feature matching results in a lot of false alarms. To overcome the mentioned problem, we propose to use mutual information (MI) along with the SIFT operator using wavelet-based hierarchical pyramid.

MI is an established registration similarity metric and has the capability to quickly estimate rough registration parameters from down-sampled images [13]. The rough registration parameters obtained using MI can be introduced for conjugate feature selection during the SIFT matching phase at the first pyramid level. Introduction of MI to the SIFT processing chain not only reduces the number of false alarms drastically but also helps to increase the number of matches as the operator detection and matching thresholds can be relaxed, relying on the available mutual information estimate.
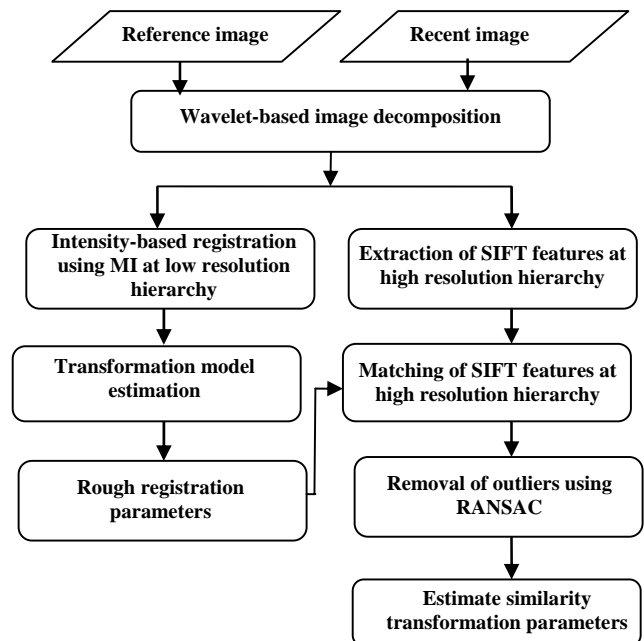
Fig. 3 Framework for proposed wavelet-based hybrid image registration methodology.

7.1 Mutual-Information-Based Registration

The idea here is to quickly estimate rough registration parameters at highest wavelet-based pyramid level and then select only those SIFT matches extracted from lowest pyramid level images where conjugate features are within a user defined threshold from the approximated rough registration parameters.

At the second level of the pyramid, a similarity (linear conformal) transformation between the approximation coefficients of both reference and recent images was applied. It was used to correct rotation, translation, and scaling displacements between the images.

In 2D, a similarity transformation model, which has four degrees of freedom, can be written as [14]:

$$\begin{bmatrix} x_2 \\ y_2 \end{bmatrix} = s \begin{bmatrix} \cos\theta & -\sin\theta \\ \sin\theta & \cos\theta \end{bmatrix} \begin{bmatrix} x_1 \\ y_1 \end{bmatrix} + \begin{bmatrix} d_x \\ d_y \end{bmatrix} \tag{9}$$

where s, θ, (d_x, d_y) are the scaling, rotation, and translation parameters, respectively.

7.2 SIFT-Based Image Registration

As explained above, the matching threshold is calculated as the ratio between Euclidean descriptor distance between the second-closest and the closest match of a feature. At a matching threshold (t) of 1.0, the rough registration parameters was utilized to compute an approximate match region for every match and filter out those matches where corresponding feature did not lie within a user defined window size (16 pixels). In general, the SIFT operator matching scheme leads to large number of false alarms as the matching thresholds are relaxed and thus some kind of a filtering to remove the outliers is absolutely mandatory. The RANSAC algorithm has been utilized to filter SIFT matched features and estimate final similarity transformation parameters.

Fig. 4 and Fig. 5 illustrate typical examples of registration results using image registration techniques in the spatial domain and in the wavelet domain, for both dental panoramic X-ray images and brain MR images. It has been shown that registered images in the wavelet domain is better than those in the spatial domain. It can be seen that after registration using cross-correlation, SIFT features, and hybrid registration technique described in [7] combining MI at down sampled images and SIFT operator in the spatial domain using rigid transformation (rotation and translation only), there were still a considerable amount of misregistration visible in the difference image. It can be shown that registered images using MI-based hierarchical registration were not clear. However, after proposed wavelet-based hybrid technique, the amount of misregistration visible in the difference images have been reduced significantly.

8. Measures of Performance

Two statistical performance measures have been used as an evaluation tool for registration quality: normalized cross-correlation coefficient (NCCC) and percentage relative root mean square error (PRRMSE).

8.1 Normalized Cross-Correlation Coefficient (NCCC)

The normalized cross-correlation coefficient (NCCC) was calculated between every reference image and registered image such that [15]:

$$NCCC = \frac{\sum_{j,k} [I_{ref}(j,k) - \bar{I}_{ref}][I_{reg}(j,k) - \bar{I}_{reg}]}{\left\{ \sum_{j,k} [I_{ref}(j,k) - \bar{I}_{ref}]^2 \sum_{j,k} [I_{reg}(j,k) - \bar{I}_{reg}]^2 \right\}^{0.5}} \tag{10}$$

where I_{ref} and I_{reg} refer to reference and registered images, with means $\bar{I}_{ref}$ and $\bar{I}_{reg}$, respectively, while j, k are the pixel coordinates. The average NCCC was calculated for each registration technique.

8.2 Percentage Relative Root Mean Square Error (PRRMSE)

In order to investigate the performance of each registration technique, the percentage root mean square error relative to reference image (PRRMSE) was calculated for each case such that [16]:

$$PRRMSE = \sqrt{\frac{\frac{1}{JK}\sum_{j=1}^{J}\sum_{k=1}^{K}\left(I_{reg}(j,k) - I_{ref}(j,k)\right)^2}{\sum_{j=1}^{J}\sum_{k=1}^{K} I_{ref}(j,k)}} * 100 \tag{11}$$

9. Results

Table 1 depicts the performance evaluation results obtained before and after applying proposed registration techniques in the spatial domain and in the wavelet domain, for 25 dental panoramic X-ray image pairs and 27 brain MR image pairs. It can be seen that results of registration techniques in the wavelet domain is better than those in the spatial domain except cross-correlation based registration technique using brain MR images, the results are approximately the same. It has been shown that

registration using cross-correlation and SIFT features gave the worst performance results for both NCCC and PRRMSE. Cross-correlation based registration was easy to implement but it has been found that it works well if only a translation motion is present between two registered images. Registration using SIFT features was influenced by large number of false alarms obtained at SIFT features matching scheme.

Registration using hybrid approach combining MI and SIFT in the spatial domain with rigid transformation [7] did not provide good registration results. MI-based hierarchical registration reported values for NCCC and PRRMSE of 0.7947 and 0.1024% respectively, for dental panoramic X-ray images and 0.9340 and 0.0246% respectively, for MR images of the brain. Wavelet-based registration technique combining MI and SIFT operator utilized in the present work gave NCCC and PRRMSE of 0.7805 and 0.1040% respectively, for dental panoramic X-rays and 0.9303 and 0.0259% respectively, for brain MR images. It can be seen that there was not significant differences between results of MI-based registration and proposed hybrid technique. However, it can be noted that registration by maximization of MI was computationally expensive. The results of NCCC, PRRMSE and visual inspection using obtained difference images demonstrated a superior performance of proposed wavelet-based registration technique combining MI, SIFT operator, and RANSAC algorithm.

10. Conclusion and Future Work

In this work, four image registration techniques are utilized in the wavelet domain to register dental panoramic X-ray images and MR images of the brain. These are: cross-correlation based image registration, registration using SIFT features, and mutual-information-based hierarchical registration, and hybrid registration technique combined with wavelet-based hierarchical strategy. The fourth technique presented a combination of mutual information and SIFT operator. At highest wavelet-based pyramid level, mutual-information-based registration was applied and rough similarity transformation parameters were achieved. At first decomposition level, scale invariant feature transform (SIFT) based registration was utilized using rough parameters obtained from MI. A RANdom Sample And Consensus (RANSAC) algorithm was applied to filter SIFT matched features and estimate final similarity transformation parameters.

A comparison between results obtained from proposed techniques with hybrid registration technique combining MI and SIFT operator in the spatial domain [7] with rigid transformation and with three registration techniques in the spatial domain was performed. Performance evaluation of the proposed registration techniques was calculated using:

normalized cross-correlation coefficient (NCCC) and percentage relative root mean square error (PRRMSE). Applying different registration techniques to dental panoramic X-ray images and brain MR images has proven that proposed wavelet-based hybrid registration technique combining MI, SIFT operator, and RANSAC algorithm is an effective tool for registration of two types of images. It gave the best results for NCCC and PRRMSE. It gave 0.7805 NCCC, and 0.1040% PRRMSE, for dental panoramic X-ray images, while 0.9303 NCCC and 0.0259% PRRMSE, for MR images of the brain. Our on-going research includes: conducting a more extensive set of tests such as liver CT images, trying to improve the efficiency of the registration results using SIFT with principal component analysis (PCA) algorithm, and applying another outlier detector technique using Hough transform.

References

[1]   Y.M. Zhu and S.M. Cochoff, "An object-oriented framework for medical image registration, fusion, and visualization," *Computer Methods and Programs in Biomedicine*, vol. 82, pp. 258-267, 2006.

[2]   X.Y. Wang, D.D. Feng, and H. Hong, "Novel elastic registration for 2D medical and gel protein images," *APBC'03*, vol. 19, pp. 223-226, 2003.

[3]   X. Wang and D.D. Feng, "Automatic hybrid registration for 2-dimensional CT abdominal images," Third International Conference for Image and Graphics,Australia, pp. 208-211, December 2004.

[4]   D.G. Lowe, "Object recognition from local scale-invariant features," *International Conference on Computer Vision, Corfu, Greece*, pp. 1150 -1157, September 1999.

[5]   D.G. Lowe, "Distinctive image features from scale-invariant keypoints, " *International Journal of Computer Vision*, vol. 60, no. 2, pp. 91-110, 2004.

[6]   E.I. Zacharaki and D. Shen, "ORBIT: A multiresolution framework for deformable registration of brain tumor images," *IEEE Trans. on Medical Imaging*, vol. 27, no. 8, pp. 1003-1017, August 2008.

[7]   S. Suri, P. Schwind, P. Reinartz, and J. Uhl, "Combining mutual information and scale invariant feature transform for fast and robust multisensor SAR image registration," *Proc. of the 75th ASPRS Annual Conference, Batlimore, Maryland, USA*, 2009.

[8]   J. P. Lewis, Fast Template Matching. Vision Interface, pp. 120-123, 1995.

[9]   S. Veeser, M.J. Dunn, and G.Z. Yang, "Multiresolution image registration for two-dimensional gel electrophoresis," *Proteomics*, vol. 1, pp. 865-870, 2001.

[10] S. Gefen, O. Tretiak, and J. Nissanov, "Elastic 3-D alignment of rat brain histological images," *IEEE Trans. on Medical Imaging*, vol. 22, no. 11, pp. 1480-1489, November 2003.

[11] J.P.W. Pluim, J.B.A. Maintz, and M.A. Viergever, "Mutual-information-based registration of medical images: a survey," *IEEE*

Trans. on Medical Imaging, vol. 22, no. 8, pp. 987-1004, August 2003.

[12] M.A. Fischler and R.C. Bolles, "Random sample consensus: a paradigm for model fitting with application to image analysis and automated cartography," *Communications of the ACM*, vol. 24. no. 6, pp. 381-395, 1981.

[13] A.A.C. Rhodes, K.L. Johnson, J. LeMoigne, and I. Zavorin, "Multiresolution registration of remote sensing imagery by optimization of mutual information using a stochastic gradient," *IEEE Trans. on Image Processing,* vol. 12, pp. 1495-1511, 2003.

[14] L. Shang, J.C. Lv, and Z. Yi, "Rigid medical image registration using PCA neural network," *Neurocomputing*, vol. 69, pp. 1717-1722, 2006.

[15] A. Gholipour and N. Kehtarnavaz, "Brain functional localization: a survey of image registration techniques," *IEEE Trans. on Medical Imaging*, vol. 26, no. 4, pp. 427-451, April 2007.

[16] F. Laliberte, L. Gagnon, and Y. Sheng, "Registration and fusion of retinal images–an evaluation study," *IEEE Trans. on Medical Imaging*, vol. 22, no. 5, pp. 661-673, May 2003.

[17] Xu, R. and Y.W. Chen, "Wavelet-based mulitresolution medical image registration strategy combining mutual information with spatial information," *International Journal of Innovative Computing, Information and Control*, vol. 3, no. 2, pp. 285-296, April 2007.

Table 1: Results of different registration techniques for 25 dental panoramic X-ray pairs and 27 Brain MR image pairs

Image Registration Techniques			Spatial Domain		Wavelet Domain	
			Average NCCC	Average PRRMSE%	Average NCCC	Average PRRMSE%
Dental Panoramic X-rays	Before registration	X'	0.6432	0.1369	0.6432	0.1369
		SD	0.1462	0.0312	0.1462	0.0312
	Registration using cross correlation	X'	0.6992	0.1275	0.7298	0.1177
		SD	0.1247	0.0354	0.1354	0.0306
	MI-based registration	X'	0.7840	0.1055	0.7947	0.1024
		SD	0.0861	0.0210	0.0763	0.0179
	Registration using SIFT features	X'	0.7020	0.1201	0.7181	0.1224
		SD	0.1114	0.0191	0.1118	0.0386
	Hybrid registration technique [6]	X'	0.7124	0.1204	---	---
		SD	0.1291	0.0285	---	---
	Proposed Technique	X'	---	---	0.7805	0.1040
		SD	---	---	0.0878	0.0183
Brain MR Images	Before registration	X'	0.8342	0.0402	0.8342	0.0402
		SD	0.0469	0.0095	0.0469	0.0095
	Registration using cross-correlation	X'	0.9030	0.0305	0.9019	0.0307
		SD	0.0371	0.0072	0.0372	0.0073
	MI-based registration	X'	0.9250	0.0271	0.9340	0.0246
		SD	0.0244	0.0082	0.0176	0.0055
	Registration using SIFT features	X'	0.8964	0.0312	0.9077	0.0301
		SD	0.0367	0.0089	0.0517	0.0099
	Hybrid registration technique [6]	X'	0.8839	0.0333	---	---
		SD	0.0516	0.0098	---	---
	Proposed Technique	X'	---	---	0.9303	0.0259
		SD	---	---	0.0245	0.0069
X'=mean				SD=standard deviation		
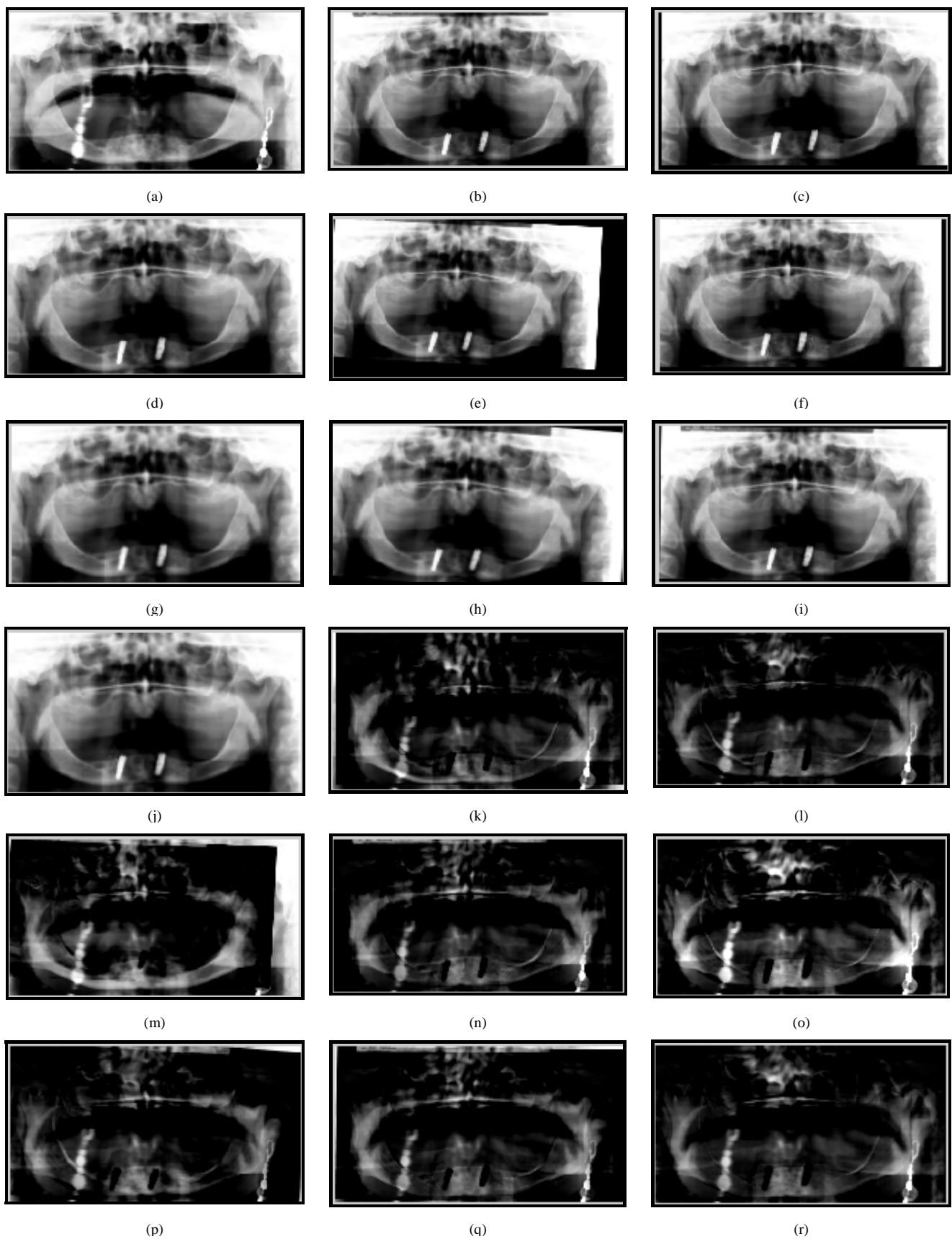
Fig. 4 The registered images using (c) cross-correlation, (d) MI, (e) SIFT features in the spatial domain, (f), (g), (h) the corresponding registered images in the wavelet domain, (i) hybrid [7], and (j) proposed wavelet-based hybrid registration techniques for a dental X-ray (a) reference image and (b) recent image. The corresponding difference images are shown form (k)-(r), respectively.
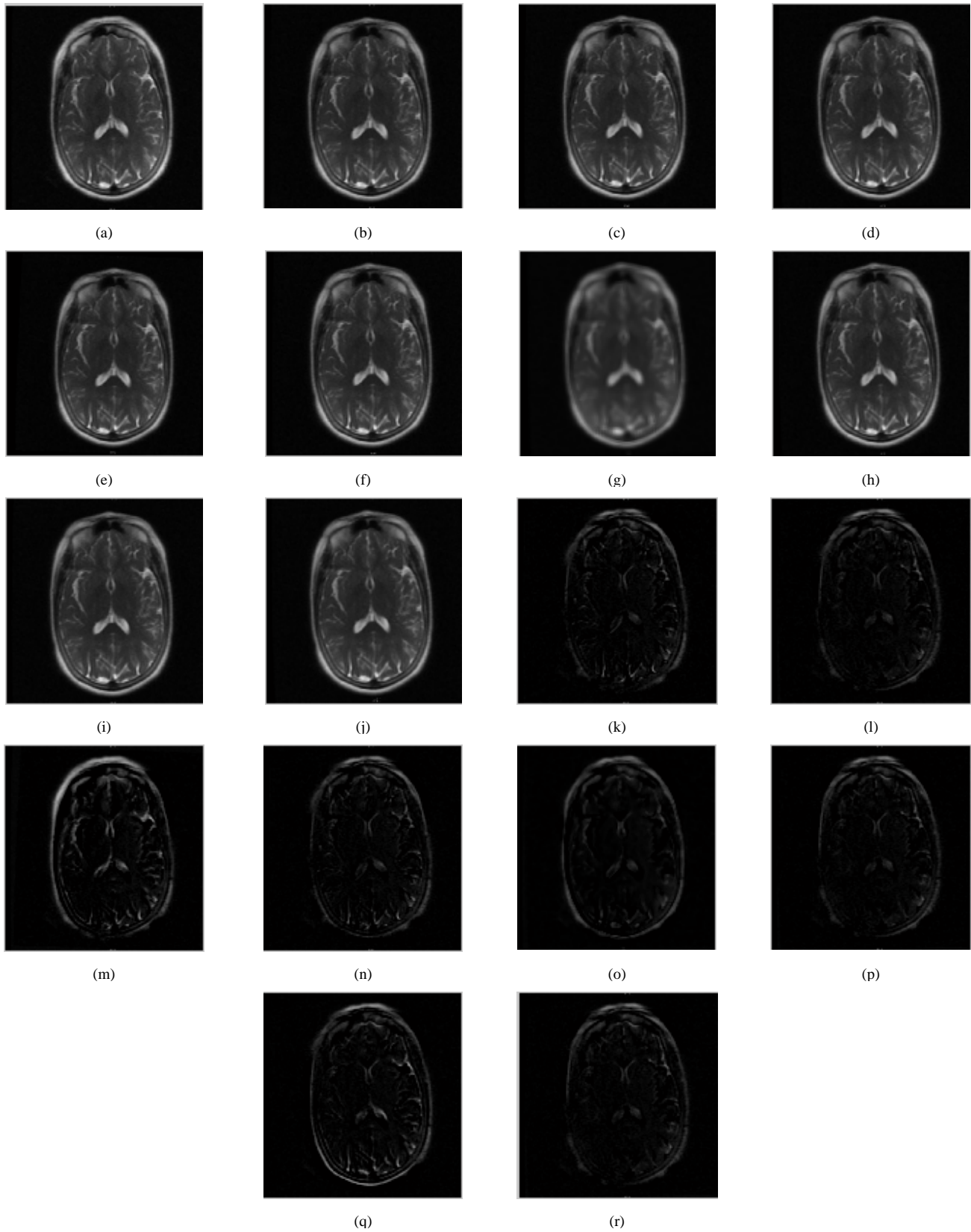
Fig.5 The registered images using (c) cross-correlation, (d) MI, (e) SIFT features in the spatial domain, (f), (g), (h) the corresponding registered images in the wavelet domain, (i) hybrid [7], and (j) proposed wavelet-based hybrid registration techniques for a brain MR (a) reference image and (b) recent image. The corresponding difference images are shown form (k)-(r), respectively.